

QUARTERLY JOURNAL  
OF THE  
ROYAL METEOROLOGICAL SOCIETY

Vol. 123

APRIL 1997 Part A

No. 539

*Q. J. R. Meteorol. Soc.* (1997), **123**, pp. 537–559

Numerical simulation of an extreme rainfall event in Catalonia: Role of  
orography and evaporation from the sea

By ROMUALDO ROMERO, CLEMENTE RAMIS\* and SERGIO ALONSO

*Universitat de les Illes Balears, Spain*

(Received 2 November 1995; revised 24 June 1996)

SUMMARY

During the evening of 12 November 1988, heavy rainfall occurred in Catalonia (north-east Spain); as a result there was flooding and heavy loss. In this paper we present a 12-hour numerical simulation of that event by means of a meso- $\beta$  scale numerical model. The results show that the model is capable of giving the localization of observed precipitation satisfactorily, but it underestimates the amount of rainfall. Other numerical experiments were done to show the effects of orography and evaporation from the Mediterranean. The effect of orography is decisive as regards the spatial structure of precipitation over land, since it acts to concentrate the precipitation in the coastal zone. The effect of evaporation from the sea is very weak, probably on account of the shortness of the simulation.

KEYWORDS: Heavy rain Western Mediterranean Mesoscale numerical prediction

1. INTRODUCTION

During the evening and early night of 12 November 1988, there was heavy rainfall in Catalonia, a coastal region located in the north-eastern part of Spain (Fig. 1). Floods occurred as a consequence of some rivers overflowing. Eleven people lost their lives and damage was calculated at around 20 million ECUs<sup>†</sup>.

The Spanish Mediterranean coastal region is commonly affected by heavy rain, on average several times a year. These events take place mostly during the autumn and usually cause local flooding. In fact, daily rainfalls exceeding 200 mm have been recorded at most of the observatories in Catalonia and the Valencia region (Font 1983), and, during the last ten years, there have been catastrophic floods every year in these coastal regions. As examples of extreme rainfall, 800 mm was recorded in the space of 24 hours in Gandía (Valencia) on 3 November 1987 and more than 400 mm in L'Alforja (Catalonia) on 10 October 1994.

Two recent studies can be quoted as representative of the state of the art in the diagnosis of extreme-rainfall episodes in eastern Spain. Ramis *et al.* (1994) concentrate on identifying the synoptic and mesoscale mechanisms responsible for the floods of October 1987 in Catalonia. Ramis *et al.* (1995) compared the heavy rains in Catalonia of October 1987 with those of November 1988. Using objective diagnosis, they identified a common scenario in both cases: moisture convergence in the lowest 1500 metres, upward quasi-geostrophic forcing at 850 hPa and convective instability over an area very close to Catalonia. Moreover, the convective available potential energy (CAPE) exceeded 2250 J kg<sup>-1</sup> in both events when

\* Corresponding author: Universitat de les Illes Balears, Grup de Meteorologia, Facultat de Ciències, 07071 Palma, Spain.

<sup>†</sup> European Currency Units.

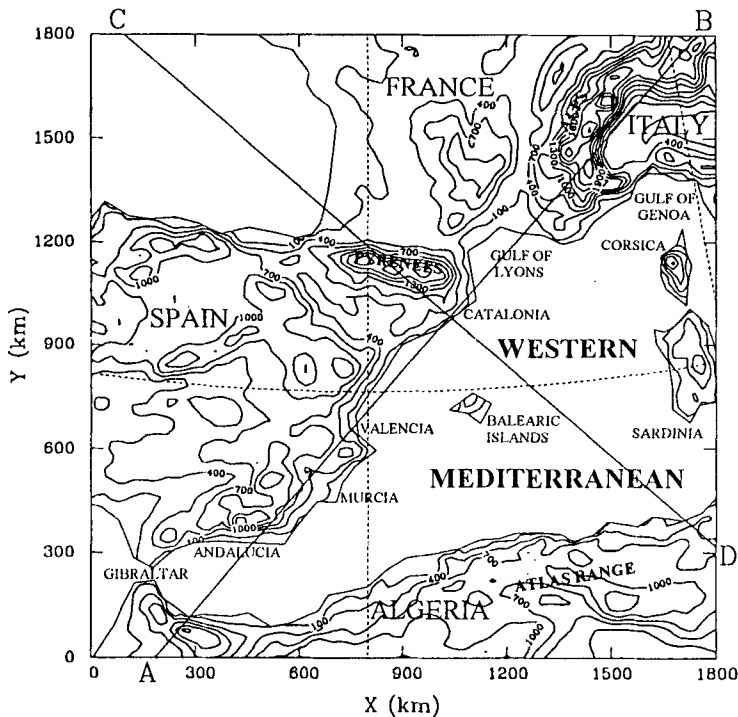


Figure 1. The western Mediterranean region showing the orography (contour interval is 300 m starting at 100 m) and the sites mentioned in the text. The area corresponds to the domain for the simulations and includes the cross-sections AB, CD referred to in the text.

the heavy rain occurred. A comprehensive list of references related to heavy rains in the Mediterranean can be obtained from these two publications.

In this paper, we study once again the extreme event that occurred in Catalonia on 12 November 1988. However, our approach differs from that of Ramis *et al.* (1995) because, in this work, we present a numerical study of the event. It should be noted that, so far, only a few numerical simulations have been done for the western Mediterranean, in spite of the advantage that numerical simulation provides in reaching a better understanding of these extreme phenomena. Studies similar to this have already been done to investigate convective heavy-rain events in the Po valley, Italy (Paccanella *et al.* 1992) and in the Valencia region (Fernández *et al.* 1995).

In this paper we have a double objective. First, we wish to study the feasibility of numerical simulations for this kind of event in the Mediterranean area, and secondly to study the effect of evaporation from the sea and of orography on the precipitation field and surface flow. This we accomplish following the methodology of Stein and Alpert (1993) and Alpert *et al.* (1995). The western Mediterranean remains still relatively warm during the autumn, so permitting intense evaporation and, therefore, the production of convective instability. Furthermore, the western Mediterranean is surrounded by mountain ranges (Alps, Pyrenees, Atlas etc.; see Fig. 1) that can interact with the synoptic flow and by so doing develop mesoscale systems. More precisely, a distinctive coastal range with altitudes of up to 1500 m can be an important factor in the development of convection in Catalonia. In previous subjective studies (e.g. García-Dana *et al.* 1982; Miró-Granada 1974; Ramis

*et al.* 1986), both evaporation from the sea and orography were considered as being the most important factors in this kind of event.

In section 2, we present an overview of the synoptic situation by way of an introduction to the subject. Section 3 describes the model that was used, and section 4 the numerical experiments that were carried out. Finally, in section 5 the results are discussed and in section 6 we give our conclusions.

## 2. SYNOPTIC OVERVIEW

The synoptic pattern at low levels for this event was dominated by an anticyclone located over the European continent, stretching as far as the western Mediterranean and producing a south-easterly flow towards the Catalan coast. A baroclinic shortwave trough, reflected as a low-pressure centre with an associated frontal system, moved towards the east from Gibraltar and was located over south-east Spain. This low-pressure centre, combined with the anticyclone, created a strong pressure gradient over the Mediterranean, with winds blowing directly towards the Catalan coast, so favouring the advection of warm humid air towards the northern part of the western Mediterranean. In Figs. 2(a) and (b), which show the meteorological situation at 1000 and 850 hPa at 12 UTC on 12 November 1988, these features are clearly visible.

At upper levels, the wave exhibited a closed circulation with a cold core over south-eastern Spain (see Fig. 2(c)), the trough having a slightly negative tilt and low cyclonic vorticity. From an inspection of Figs. 2(a), (b) and (c) and the 300 hPa chart (not shown) it seems that the vertical axis of the wave tended to tilt slightly to the south-east with height. The satellite picture at that time (Fig. 3(a)) shows clouds over Catalonia and the Mediterranean area, with a frontal band over the African coast. Convection cannot be easily observed within the general structure of the clouds but it did occur over Catalonia (as indicated by the SYNOP information).

A synoptic-scale objective diagnosis of the event was done by Ramis *et al.* (1995) who calculated the factors favourable for convective development at that scale (Barnes 1985; Barnes and Newton 1986). The diagnostic information they summarized by means of a composite chart in which were plotted the zero contours of quasi-geostrophic forcing at 850 hPa, the difference in  $\theta_e$  between 500 and 1000 hPa, and the vapour convergence in the 1000–850 hPa layer. The area where the three favourable processes overlap represents a zone where, as a consequence of the synoptic structure, mesoscale lifting mechanisms have greater facility for the development of convection. Figure 4 contains the composite chart for 12 UTC 12 November 1988. It shows that the area of overlap for the favourable mechanisms extended over the western Mediterranean as far as the Catalan coast. Satellite pictures show that convection developed during the afternoon south of the Balearic Islands and progressed northwards (see Fig. 3).

The synoptic pattern evolved in the hours following with a displacement of the low to the north, the displacement in the upper levels being much more distinct than in the lower levels. The composite chart of favourable synoptic-scale parameters for 00 UTC 13 November 1988 showed the intersection zone situated over the Mediterranean and reaching as far as the south of France. The satellite picture for that time (Fig. 3(b)) shows the cold front and the convection over the Mediterranean and Catalonia.

The total rainfall in Catalonia for the period from 07 UTC 12 November to 07 UTC 13 November was very high (see Fig. 5). Most of the precipitation fell during the evening of the 12th. It can be seen that more than 200 mm fell close to Barcelona, with a tongue of high precipitation extending to the north. The greatest quantity was collected on the coast

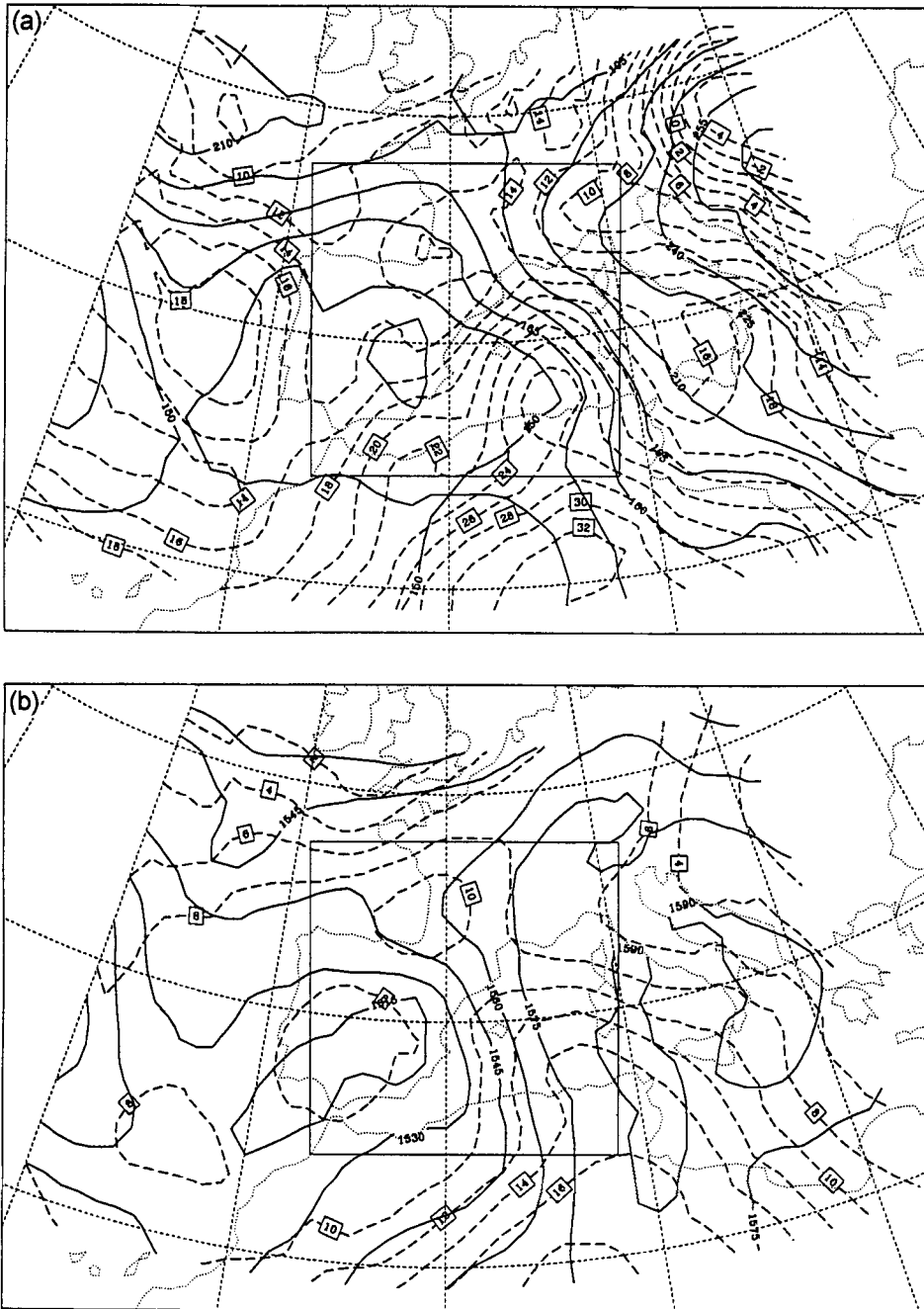


Figure 2. Synoptic situation at 12 UTC 12 November 1988, showing height (gpm, continuous line) and temperature ( $^{\circ}\text{C}$ , dashed line). (a) 1000 hPa, (b) 850 hPa, (c) 500 hPa. The central square corresponds to the domain for the simulations.

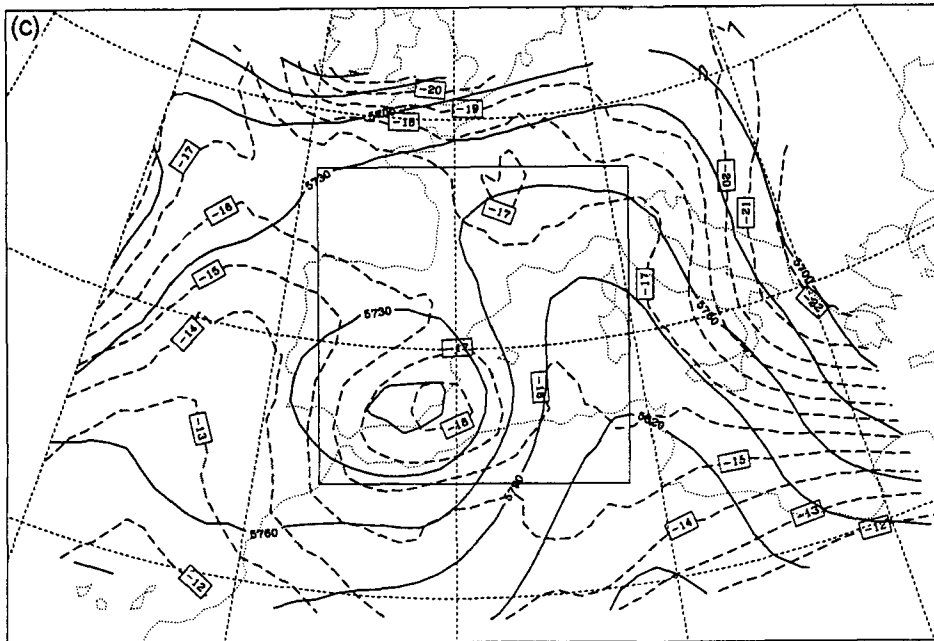


Figure 2. Continued.

and pre-coastal zone where there exists important orography (see Fig. 1). It seems quite possible, therefore, that the orography played an important part in focusing the convection.

### 3. MODEL DESCRIPTION

The simulations presented were carried out with the help of the hydrostatic, three-dimensional, meso- $\beta$  model developed by Nickerson *et al.* (1986), the model equations being expressed in a terrain-following coordinate system in which the vertical coordinate  $\nu$  is related to the usual coordinate  $\sigma$  by the expression

$$\sigma = \frac{1}{3}(4\nu - \nu^4).$$

In spite of working with an uniform numerical grid, the vertical resolution of the planetary boundary layer (PBL) is increased with the aid of the  $\nu$  coordinate.

The model has shown its ability to simulate a wide range of mesoscale circulations, for example, mesoscale flows induced by vegetation or soil moisture inhomogeneities (Mahfouf *et al.* 1987a; Pinty *et al.* 1989), down-slope wind storms (Richard *et al.* 1989), mountain waves (Nickerson *et al.* 1986; Romero *et al.* 1995), or the breeze circulation (in Florida: Mahfouf *et al.* 1987b; in Mallorca: Ramis and Romero 1995).

#### (a) Parametrizations

Warm microphysics is represented in the model developed by Nickerson *et al.* (1986). Both rainwater mixing ratio and raindrop concentration are predicted by the microphysical equations from which autoconversion, self-collection, accretion, evaporation and sedimentation processes are calculated on the basis of a log-normal raindrop distribution.

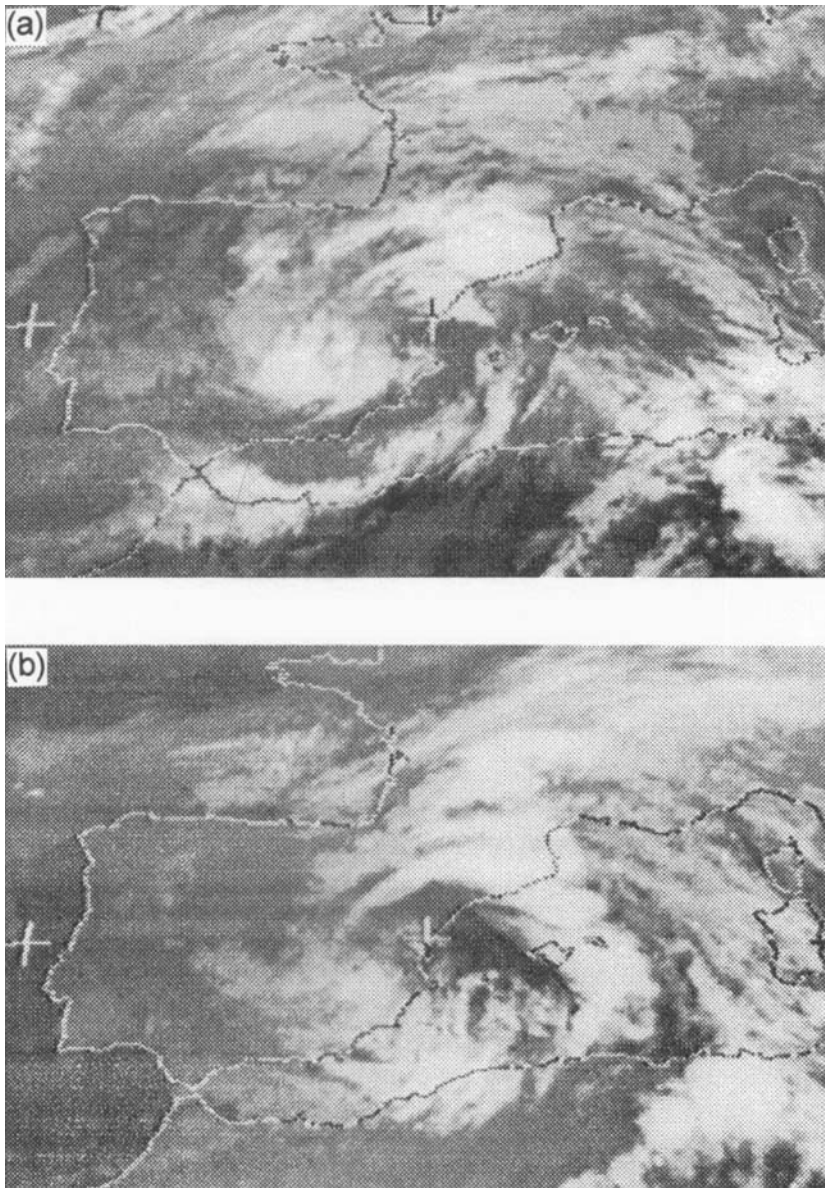


Figure 3. Infrared Meteosat image for (a) 12 UTC 12 November 1988, (b) 00 UTC 13 November 1988.

Since the type of event being studied is dominated by deep convection, the cumulus convection scheme of Emanuel (1991) has been included among the model parametrizations. This scheme is based on the dynamics and microphysics of convection as revealed from aircraft observations, the fundamental entities for moist convective transports being the subcloud-scale draughts rather than the clouds themselves. Unlike other schemes based on bulk-entraining plumes (e.g. Fritsch and Chappell 1980, Arakawa and Schubert 1974), in this scheme the convective transports are idealized, based on reversible ascent

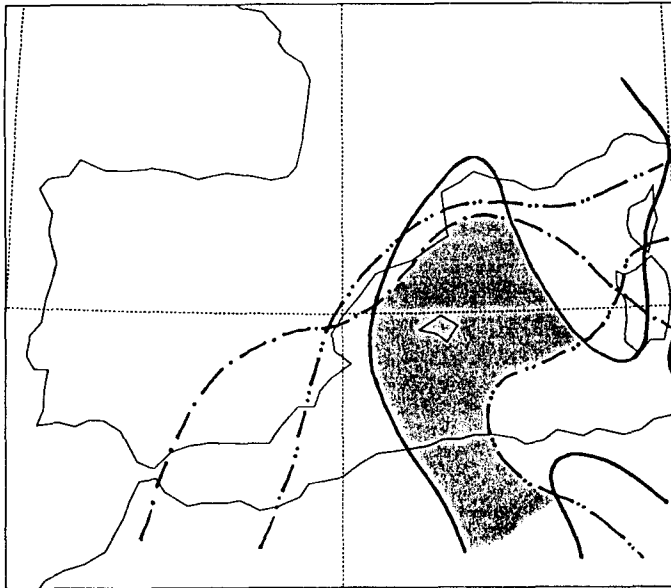


Figure 4. Composite chart for 12 UTC 12 November 1988 (after Ramis *et al.* 1995). Continuous line, zero contour of quasi-geostrophic forcing,  $FQ$ , at 850 hPa. Dot-dashed line, zero contour of equivalent potential temperature difference,  $\Delta\theta_e$ , between 500 and 1000 hPa. Dot-dot-dashed line, zero contour of moisture convergence,  $F_q$ , in the 1000–850 hPa layer. The shaded zone denotes existence of the three forcing mechanisms ( $FQ > 0$ ,  $\Delta\theta_e < 0$ ,  $F_q > 0$ ).

of the subcloud-scale entities, mixing, and buoyancy sorting (Raymond and Blyth 1986), the updraught mass fluxes being calculated as a function of CAPE in such a way as to drive the mass fluxes towards a state of quasi-equilibrium with the large-scale (explicitly resolved) forcing.

Horizontal diffusion is introduced explicitly by a fourth-order operator. The vertical turbulent mixing is expressed through an eddy-diffusivity assumption with a 3/2 order closure: the exchange coefficients are calculated as functions of the turbulent kinetic energy (predicted by the model), and the mixing-length scale after Therry and Lacarrère (1983) and Bougeault and Lacarrère (1989).

At the surface, turbulent fluxes of momentum, heat and moisture are calculated following Louis (1979). A two-layer force-restore method (Bhumralkar 1975; Blackadar 1976) has been included in the model to account for the surface temperature variation. The surface properties such as albedo, emissivity, roughness, thermal inertia and available moisture are all specified by the same surface index under the assumption that these properties appear related for natural surfaces (Benjamin and Carlson 1985). Although simple, it is possible with this method to represent the effect of surface heterogeneities on atmospheric circulations (Benjamin and Carlson 1985) sufficiently well given the lack of a flexible data-base of surface parameters specified for the purpose of running a more complete surface package.

Solar and infrared fluxes through the atmosphere, which determine the net radiation at the surface and contribute to the diabatic term of the thermodynamical equation by the flux divergence, are calculated based on the method given by Mahrer and Pielke (1977). Scattering and absorption of solar radiation by permanent gases such as oxygen, ozone and carbon dioxide are included, as is also absorption and longwave emission by the

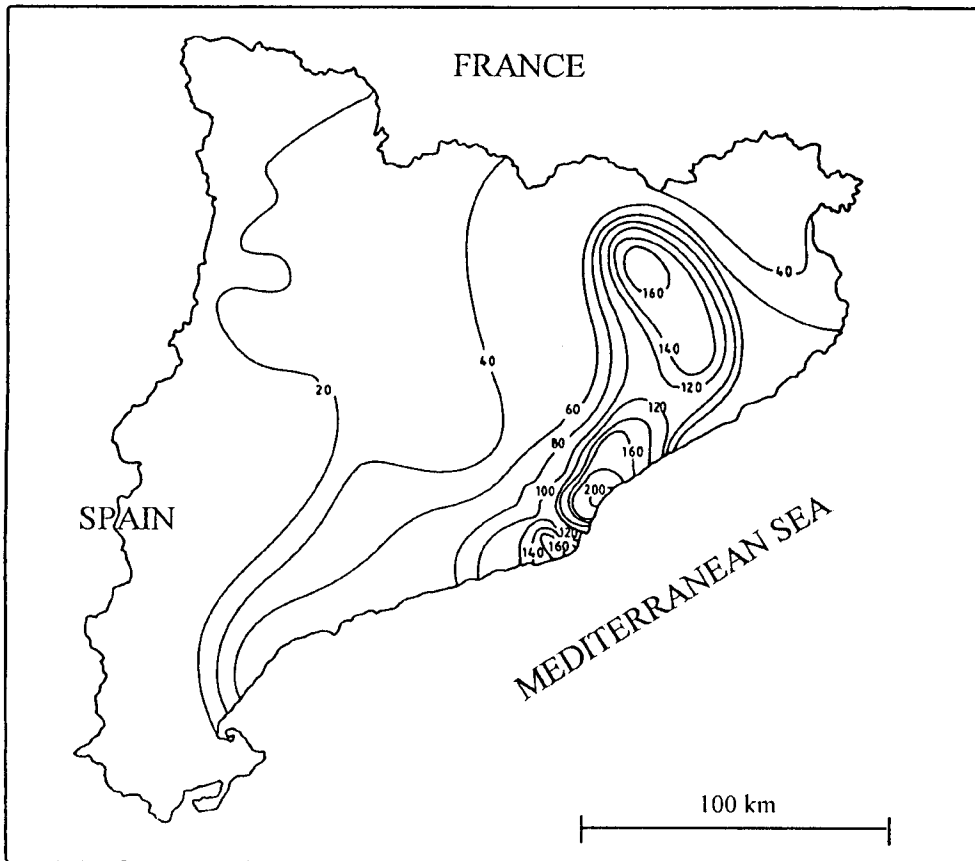


Figure 5. Total precipitation (mm) in Catalonia for the period from 07 UTC 12 November to 07 UTC 13 November.

atmospheric water constituents (water vapour and clouds). The surface radiative fluxes are modified to take the slope of the terrain into account.

(b) *Initialization and boundary conditions*

The orographic data-base (US Navy Orography), and large-scale meteorological fields in the form of uninitialized analyses on standard pressure levels for the limited area model (LAM) of the Instituto Nacional de Meteorología (INM) of Spain, are given on regular latitude–longitude grids with grid intervals of 5 minutes and 0.91 degrees, respectively. The data are initialized on the regular two-dimensional model grid, where a polar-stereographic projection is used to map the region of interest.

The orographic data are interpolated linearly to the model grid points. The short wavelength components of the interpolated orography are filtered (Shapiro 1970).

The large-scale meteorological fields comprise temperature, relative humidity, geopotential and wind components. In the case of temperature and humidity, the fields are analysed at the model grid points on the pressure surfaces by a univariate method of successive corrections (Pedder 1993).

For the wind and geopotential fields, a mass–wind balance is imposed in which the geopotential is made to adjust to the ‘observed’ wind field—a process which is applied in two steps. In the first step, the stream function and wind (including a divergent component)

are analysed for each isobaric surface, applying the statistical technique of Pedder (1989) on the wind data. This technique avoids the need for the empirical specification of external boundary conditions for the stream function and velocity potential, which is necessary in those other methods where the wind components are derived from estimated values of vorticity and divergence. In the second step, we follow Warner *et al.* (1978) and calculate the geopotential,  $\phi$ , from the stream function,  $\psi$ , by solving the balance equation

$$\nabla^2\phi = f(\psi_{xx} + \psi_{yy}) - 2m^2(\psi_{xy}^2 - \psi_{xx}\psi_{yy}) + f_y\psi_y + f_x\psi_x$$

where  $m$  is the map factor,  $f$  the Coriolis parameter, and subscripts indicate derivatives. The boundary values of  $\phi$  are given by direct analysis of geopotential data.

Sea-level data we have extrapolated from the 1000 hPa level, assuming a standard temperature lapse rate and constant relative humidity. The pressure is found hydrostatically and the wind is set to zero. Once the analysed fields are interpolated at the  $\nu$ -levels of the mesoscale model, a hydrostatic adjustment is applied through a variational method, correcting the profiles of geopotential and temperature for each grid point. The wind, which is interpolated linearly with the already corrected values of geopotential to preserve the mass–wind balance, is also slightly modified after applying a variational adjustment that minimizes the vertical integral of the horizontal divergence (Pinty 1984). The aim of this dynamic adjustment is to filter out the fast gravity waves.

At the top of the model, the vertical velocity,  $\dot{\nu}$ , is set to zero. To minimize reflection from the upper boundary, an absorbing layer is introduced in which the background diffusion (imposed by a second-order operator in this layer) is progressively increased, reaching its maximum value at the uppermost level.

One-way nesting of the mesoscale model allows assimilation of the external forcing, which is given by time-dependent prescribed values of the fields at the lateral boundaries. At any given time, the fields at the boundaries are determined by linear interpolation between the values corresponding to the available analysis times. The interior values of the fields are relaxed to the boundary values by the method used by Davies (1976).

#### 4. DESCRIPTION OF THE EXPERIMENTS

Although the total rainfall, shown in Fig. 5, corresponds to a 24-hour period, most of it was registered during the late afternoon and early night. In which case, therefore, we considered those meteorological analyses available for 12 UTC 12 November and 00 UTC 13 November and have extended the simulations for a 12-hour period between these times.

Figure 1 shows the mesoscale model domain. It is centred in the south of Catalonia at position 1°E, 41°N and measures 1800 × 1800 km<sup>2</sup>. That region is wide enough to incorporate the major Spanish orographic systems and also those formed by the western part of the Alps. North Africa, with its important orography, is also included in this area, since the influence of the Atlas range under low-level southerly flow regimes is suspected of having an important influence on the meteorological systems that develop over the southern part of the western Mediterranean (Reiter 1975). The numerical experiments have a horizontal grid length of 20 km (91 × 91 points), and 30 vertical levels. The first atmospheric level is at a height of about 4.5 m above the ground and the lowest 2 km are covered by 12 computational levels.

Based on NOAA-AVHRR mosaics and other information, seven types of land have been considered, according to the classification done by Benjamin and Carlson (1985). The surface types in the region (Fig. 6), show a transition from dry surfaces, characteristic of Africa and the major part of Spain, to the more humid zones of western Europe and the

northern part of the Mediterranean basin. The roughness length, which is a function of soil type, has been explicitly increased in areas of elevated terrain. Sea surface temperature (SST) and subsoil temperature (both constant during the simulation) correspond to the November mean values of SST (Fig. 6) and surface air temperature, respectively.

Following Stein and Alpert (1993), to isolate the effect of  $n$  factors by means of numerical simulations, it is necessary to perform  $2^n$  simulations. Therefore, four experiments are considered necessary for our purposes. We identify as  $f_0$  the experiment without orography and without evaporation from the sea,  $f_1$  represents the simulation with orography but without evaporation,  $f_2$  without orography but with evaporation from the sea allowed, and  $f_{12}$  is the complete case with both orography and sea evaporation present; these experiments are summarized in Table 1.

The contributions associated with each factor can be written:

1. Effect of the orography  $f_1^* = f_1 - f_0$ .
2. Effect of the sea evaporation  $f_2^* = f_2 - f_0$ .
3. Effect of the interaction orography-sea evaporation  $f_{12}^* = f_{12} - (f_1 + f_2) + f_0$ .

Apart from the orography and latent-heat flux at the sea surface, which are either included, or omitted (see Table 1), the rest of the parameters are initially the same for all four experiments. It should be noted that the initial fields in experiments  $f_0$  and  $f_2$  are not entirely free of orographic influence, since they are based on observations which, of necessity, contain orographic effects.

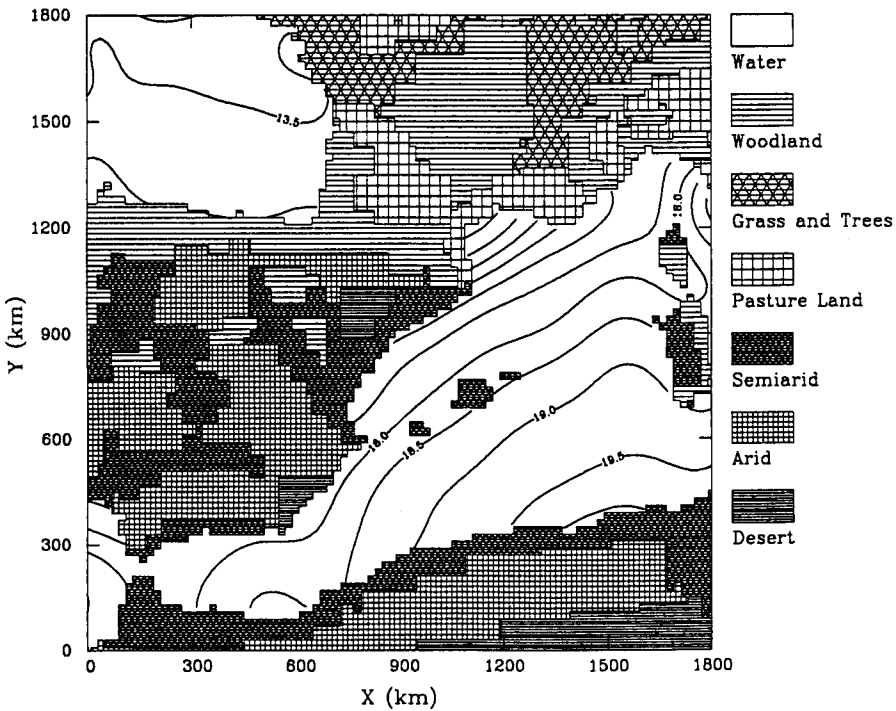


Figure 6. Distribution of surface types in the model domain and mean values of sea surface temperature ( $^{\circ}\text{C}$ ) for November.

TABLE 1. SUMMARY OF THE NUMERICAL EXPERIMENTS.

Experiment	Orography	Sea evaporation
$f_0$	NO	NO
$f_1$	YES	NO
$f_2$	NO	YES
$f_{12}$	YES	YES

These experiments were designed to isolate the effect of orography and evaporation from the sea for the case-study.

## 5. RESULTS AND DISCUSSION

### (a) *The full experiment $f_{12}$*

As already stated, a 12-hour forecast was made starting at 12 UTC 12 November 1988. In spite of the simulation being short, the spin-up process seems not to be crucial for the results, partly because of the initialization procedure applied. Twenty minutes after the simulation has started, the initial imbalances have practically disappeared. In addition, precipitation (both convective and large scale) was already occurring at the same time.

Model results at the end of the simulation (00 UTC 13 November) show that at 1000 hPa (Fig. 7(a)), a low has developed over the sea close to the Algerian coast and there is very warm air over the Mediterranean. The distribution of isotherms over the sea shows clearly a 'warm/cold' frontal structure, and the warm temperature advection seems to be large close to the Catalan coast. The isohypse distribution at 850 hPa (Fig. 7(b)) shows the low over south-east Spain, but the associated flow over the Atlas mountains is from the south, which shows that the shallow low at 1000 hPa is an orographic effect. In addition, isotherms show a foehn effect in the lee of the Atlas mountains and warm advection over the Mediterranean towards the Catalan coast.

At the 500 and 300 hPa levels (Figs. 7(c) and (d)), a low is located on the eastern coast of Spain. At the 500 hPa level the low exhibits a cold core and the closed isohypses look like a cut-off. At level 300 hPa, the thermal structure shows clearly the descent of the tropopause, especially over south-eastern Spain.

Figure 8 shows a subjective surface mesoscale analysis for 00 UTC 13 November. It should be noted that the analysis was rendered difficult in consequence of the lack of data from over the sea. When doing subjective analysis in data-sparse regions like the oceanic areas of the western Mediterranean, it is useful to apply conceptual models to help supplement the analysis. To this end we have applied models of pressure distribution around a thunderstorm (Scofield and Purdom 1986), and pressure dipole structures (high pressure on the windward side and low in the lee) such as are developed by a mountain range when wind blows normal to it, particularly in the case of southerly flows over the Alps (Vergeiner *et al.* 1982), the Pyrenees (Bessemoulin *et al.* 1993) and the Atlas mountains (Jansá *et al.* 1986). Although the data are certainly not available to validate some of the analysed structures, nevertheless we have tried to ensure that the analysis is consistent with the observations to the maximum extent possible. Thus, we believe that our subjective analysis is, at least, a plausible hypothesis about the subsynoptic-scale structure and that it is not inconsistent with the observations (including the satellite imagery shown in Fig. 3(b), and the standard synoptic data). The most salient features shown in Fig. 8 are the high pressure windward of the Alps and the low in the lee of the Atlas mountains, the

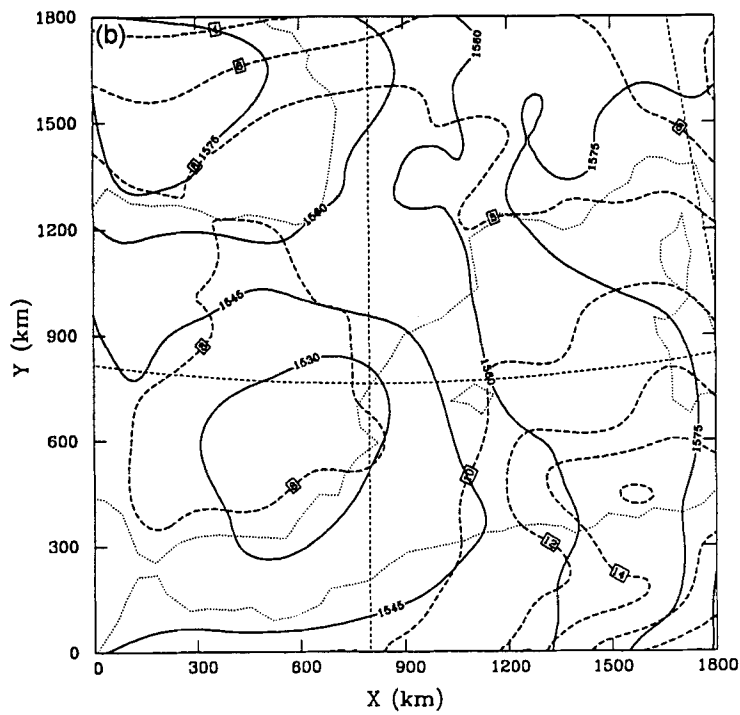
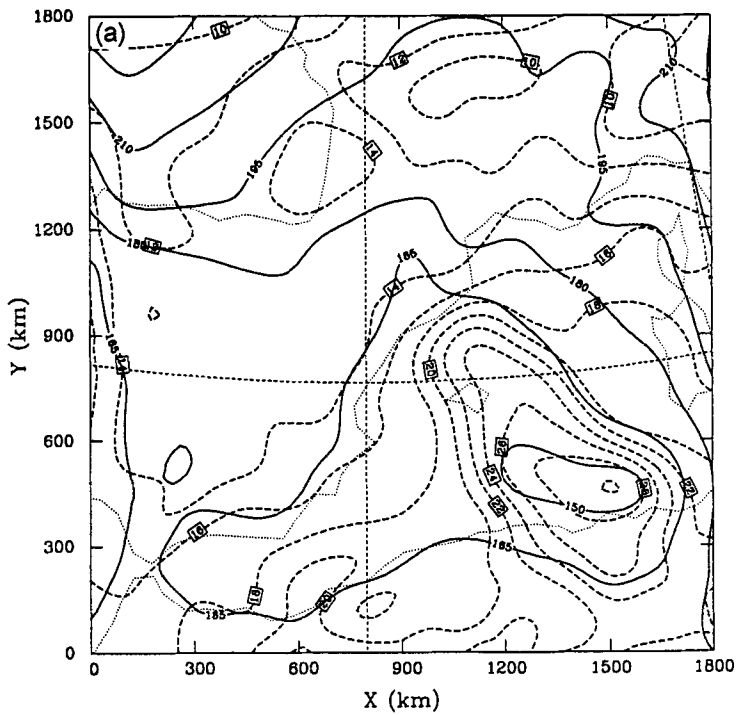


Figure 7. Forecast fields at 00 UTC, showing height (gpm, continuous line) and temperature ( $^{\circ}\text{C}$ , dashed line): (a) 1000 hPa; (b) 850 hPa; (c) 500 hPa; (d) 300 hPa.

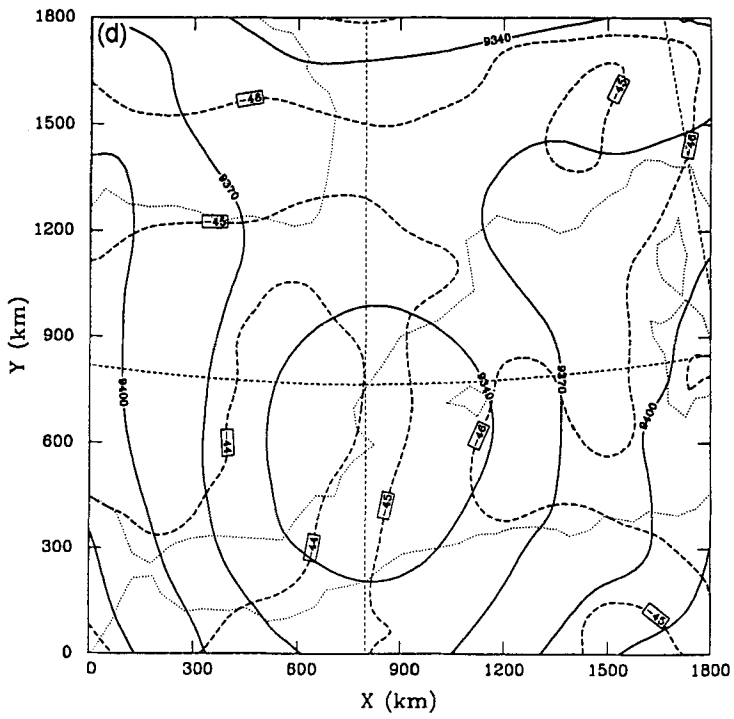
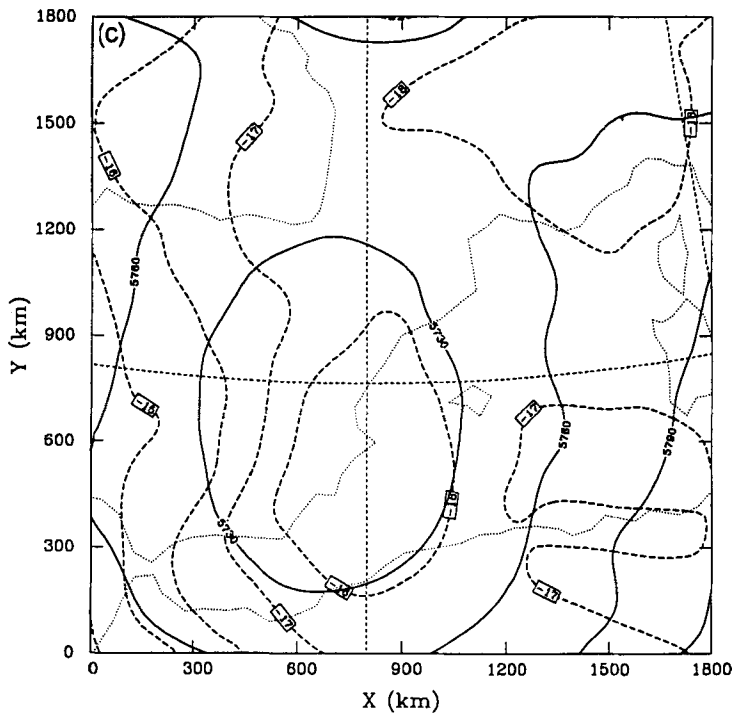


Figure 7. Continued.

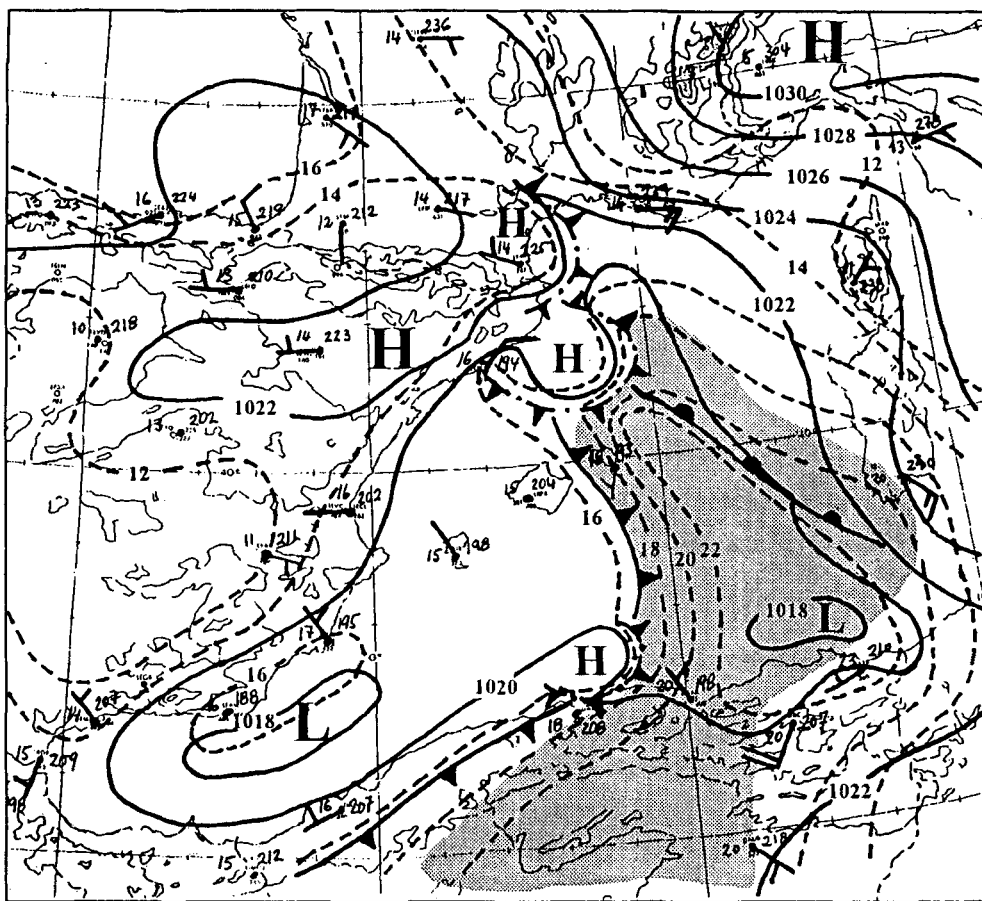


Figure 8. Subjective surface mesoscale analysis on 00 UTC 13 November 1988. Continuous lines represent isobars, dashed lines isotherms and the shaded area represents the zone with dew point higher than 16 °C. Available pressure, temperature and wind observations are plotted.

cold front on the Mediterranean and a tongue of warm moist air extending from Africa to Catalonia. A mesoscale high produced by convection close to Catalonia provides the low-level lifting mechanism for maintaining the convection over the same area. Figure 8 may be compared with the satellite image (Fig. 3(b)). The model result at 1000 hPa (Fig. 7(a)) also shows the low in the lee of the Atlas mountains and warm air over the Mediterranean; the frontal structure is also well defined. The temperatures given by the model over the Mediterranean are higher than those that can be deduced from the data used in the subjective analysis.

The forecast precipitation field is shown in Fig. 9. Figure 9(a) displays the total rainfall predicted by the model after 12 hours of simulation (00 UTC 13 November). It can be seen that the precipitation is concentrated close to the coast and over Catalonia, and also to the east of the Balearic Islands. This figure may be compared with Fig. 5 of section 2; the correspondence between the spatial distribution of rainfall over land as predicted by the model and the precipitation registered seems rather good. In particular, the observed coastal maximum is given correctly by the model. On the other hand, the model has underestimated the total precipitation.

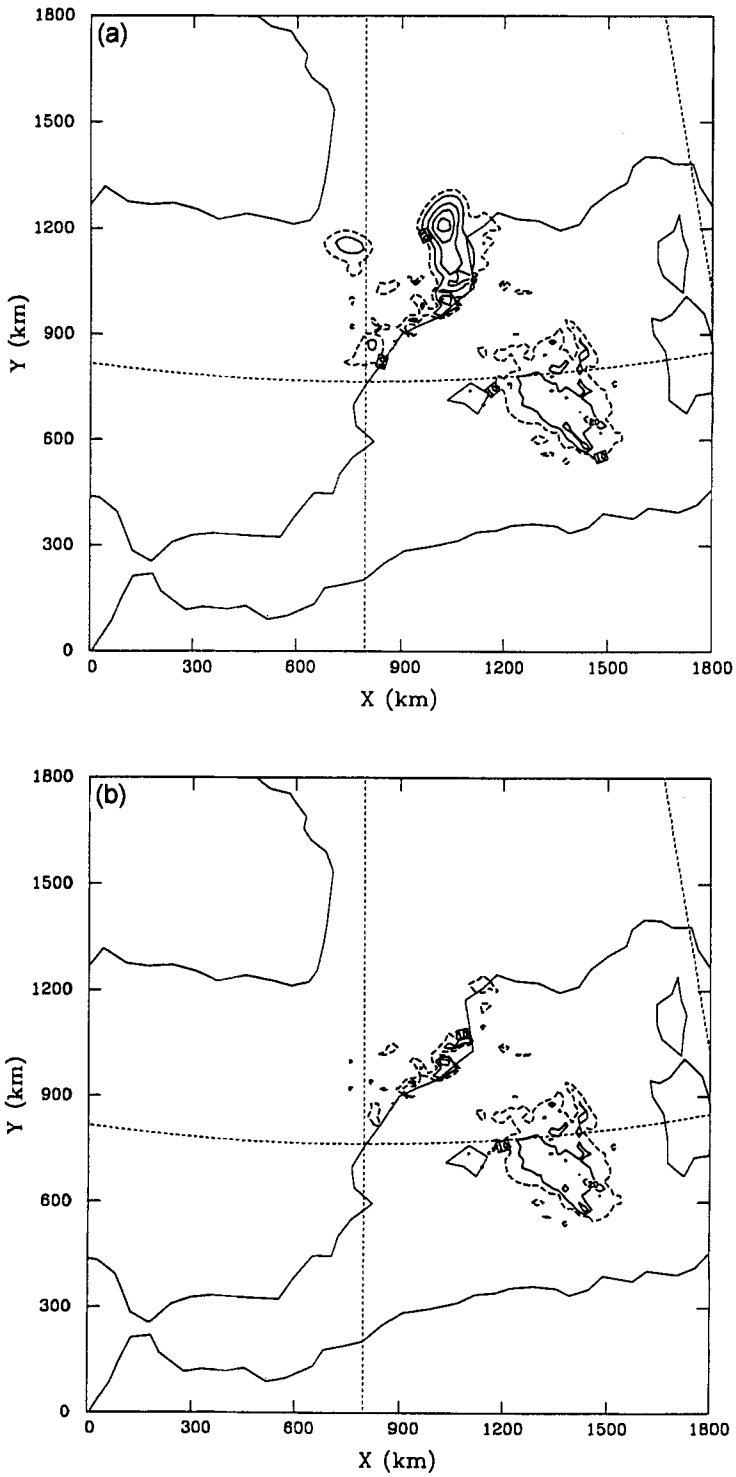


Figure 9. (a) Forecast total precipitation from 12 UTC to 00 UTC for experiment  $f_{12}$ . (b) As for 9(a), but for the convective contribution. Contour interval is 20 mm starting at 20 mm (continuous line). Dashed contour represents 10 mm.

Figure 9(b), which displays the convective part of the precipitation field, shows that the precipitation over the sea and most of the rainfall over the Catalan coast in Fig. 9(a), are given by the convective scheme.

A cross-section along direction AB in Fig. 1 (Fig. 10(a)), deduced from the 12-hour model forecast, shows that at low levels the warmest air is located close to Catalonia, while at middle tropospheric levels it is located slightly to the north-east. The equivalent potential temperature field shows that the warm air at low levels is also very humid, since there is potential instability to the south-west of, and aloft over, Catalonia up to a height of 3000 m, while at low levels over Catalonia, and to the north-east, the air is potentially stable.

Cross-section CD (Fig. 10(b)) shows also that warm air is located over the sea, to the south-east of Catalonia, where the dry static stability is very weak. In addition, isotherms of equivalent potential temperature show that the warm air is very humid at low levels, since the potential instability close to the Catalan coast is strong from the surface up to 4000 m. Therefore, the conditions for convection are found over the sea, but in close proximity to the Catalan coast.

Figure 11 shows the predicted wind field at 00 UTC at the first level (approximately 4.5 m above the ground). The strongest winds are found in the northern Mediterranean, showing strong convergence close to the north Catalan coast. Two important convergence lines appear over the sea. When they are examined in conjunction with the thermal structure at 1000 hPa (Fig. 7(a)), these are identified clearly as being associated with the frontal zones. A very small and intense cyclonic circulation appears over the Catalan coast with another (of larger diameter) between Catalonia and the Balearic Islands. The wind over Catalonia is very weak, except in the coastal zone where it is from the north and north-east. A qualitative comparison of the winds given by the model against those observed at some WMO observatories (Fig. 8) is satisfactory, and shows that along the Catalan coast, where the synoptic analysis from the LAM of the INM (not shown) gives a south-easterly wind, the model has forecasted the observed north-easterly wind well.

The latent-heat flux at the surface seems to be, *a priori*, an important factor in events of this kind, since the sea is still warm during the autumn season. Figure 12 shows the latent heat flux over the sea at 00 UTC as given by the model. Two well-defined areas of important evaporation are present. The first is located close to the Algerian coast, where the wind is appreciable and where the air is very warm and dry as a consequence of the Atlas-induced foehn. The second evaporation area is located in the northern Mediterranean, close to the French coast and coincides, again, with strong dry winds coming from the European continent.

### (b) *Effects of the orography and evaporation from the sea*

As was indicated in section 4, in the basic experiment,  $f_0$ , both the orography and latent-heat flux from the sea are omitted. The forecast precipitation field at 00 UTC is given in Fig. 13(a). It can be seen that the precipitation over the sea is similar to that obtained in the full experiment,  $f_{12}$  (Fig. 9(a)). The centre of maximum precipitation to the east of the Balearic Islands appears, but the precipitation over land is quite different.

Figure 13(b) displays the precipitation-field forecast for experiment  $f_1$ , in which the orography was included but not the evaporation. The spatial structure of the precipitation resembles that of the full experiment  $f_{12}$ , both over sea and over land. The centre of heavy precipitation over the Catalan coast is now apparent in addition to the extension of the precipitation field inland. The isolated effect of the orography ( $f_1^*$ ) is shown in Fig. 14(a). The main effect on the precipitation has been to focus it on the Catalan coast and to extend it inland. Negative contributions are noticeable only over the sea, to the east of the Balearic

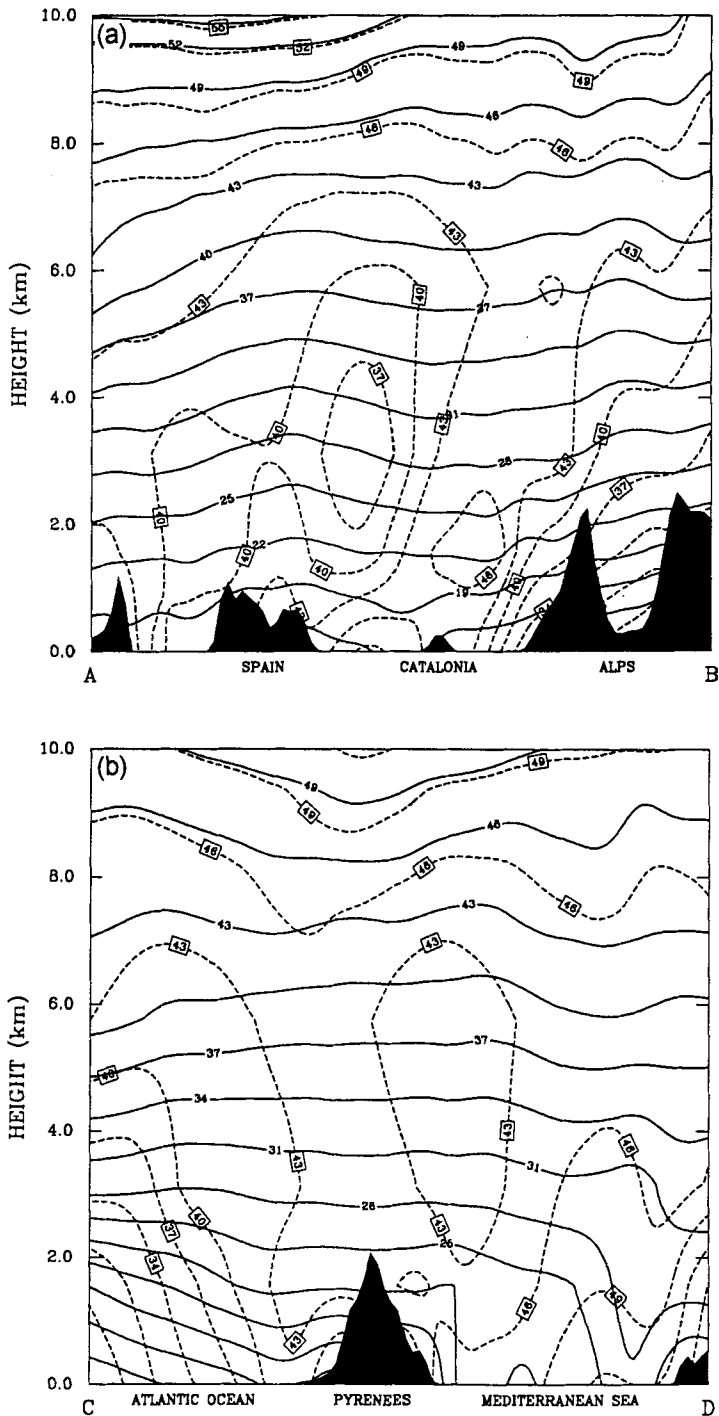


Figure 10. Thermodynamic fields given by experiment  $f_{12}$  at 00 UTC: (a) along vertical cross-section AB; (b) along vertical cross-section CD. Continuous contours represent the field of dry potential temperature ( $^{\circ}\text{C}$ ), and dashed contours of equivalent potential temperature ( $^{\circ}\text{C}$ ).

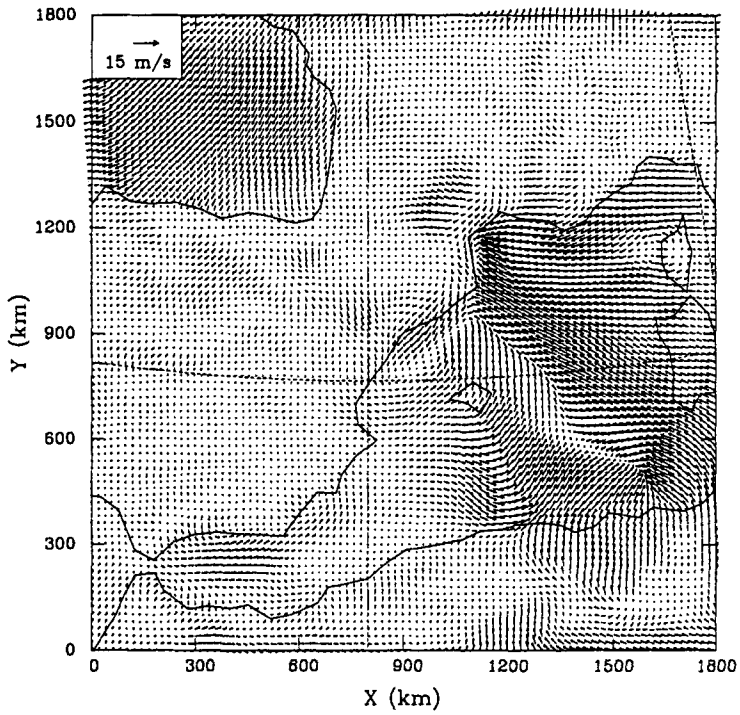


Figure 11. Forecast surface wind field at 00 UTC for experiment  $f_{12}$ . The arrow on the upper left-hand corner represents  $15 \text{ m s}^{-1}$ .

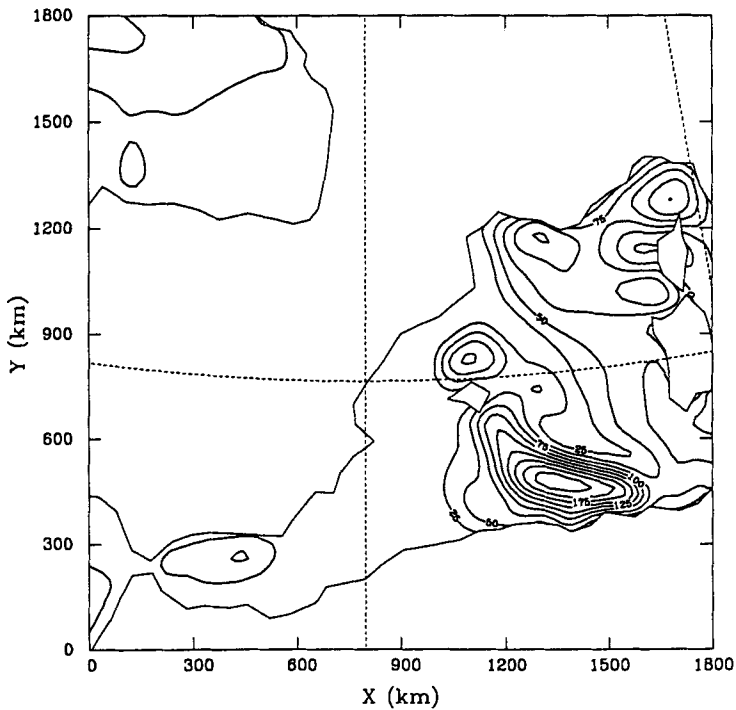


Figure 12. Latent-heat flux from the sea at 00 UTC for experiment  $f_{12}$ . Contour interval is  $25 \text{ W m}^{-2}$  starting at  $25 \text{ W m}^{-2}$ .

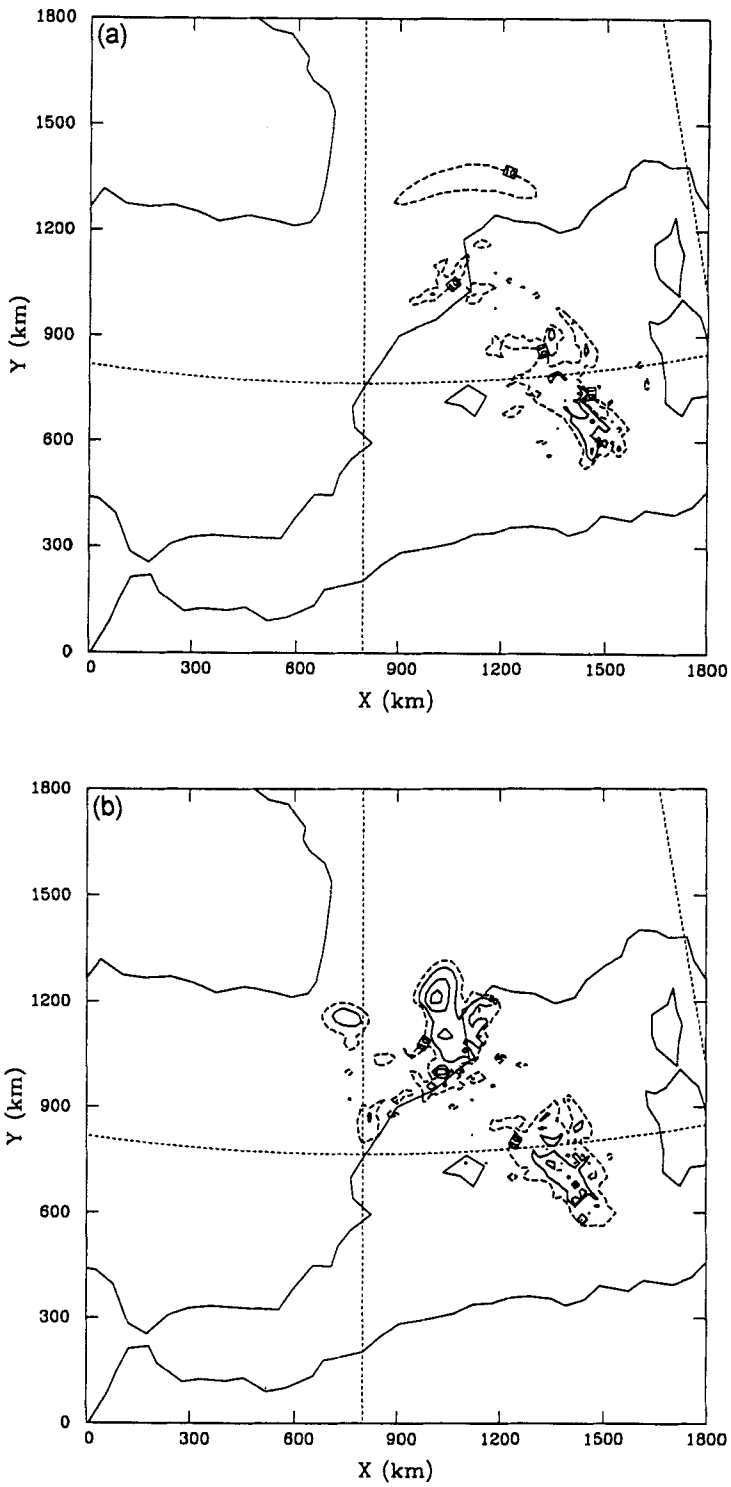


Figure 13. Forecast total precipitation from 12 UTC to 00 UTC: (a) for experiment  $f_0$ ; (b) for experiment  $f_1$ .

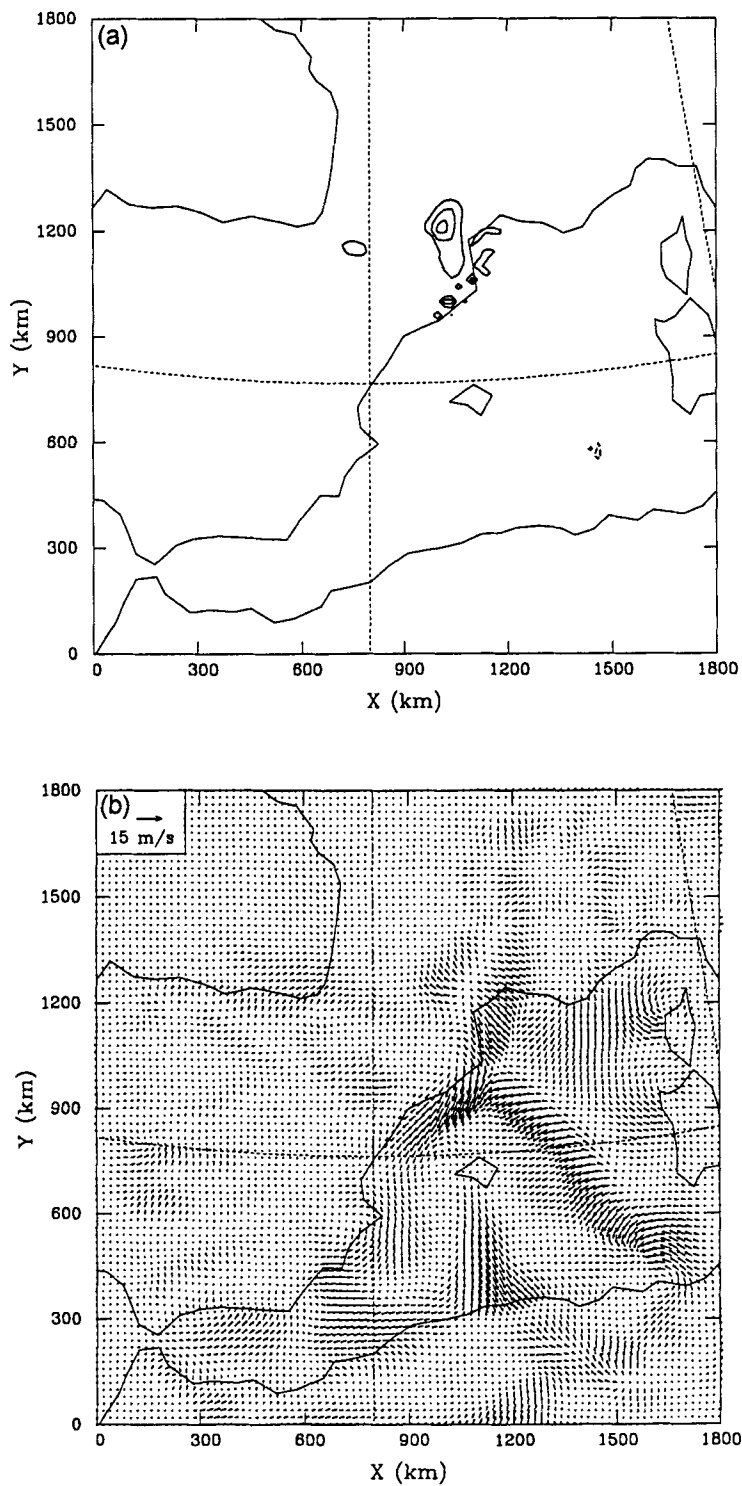


Figure 14. Effect of the orography after twelve hours of simulation (00 UTC): (a) on the total precipitation (contour interval is 20 mm starting at 20 mm, continuous line, and at -20 mm, dashed line); (b) on the surface wind field.

Islands. The effect of the orography on the wind field is shown in Fig. 14(b). The most important action appears to take place over the sea. Close to the Catalan coast the effect is very strong in the sense that it produces a backing of the wind. Close to the Algerian coast, on the eastern side of the domain, a cyclonic circulation is clearly defined extending towards the Catalan coast. Another effect can be identified close to the French coast, in the sense that the wind increases where the flow from the Gulf of Genoa ends but decreases over the coast. Similarly, the wind increases in the lee of the Pyrenees. The effect of Corsica and Sardinia is also evident; they produce in their lee, as a consequence of their shape and the atmospheric stability, circulations opposed to the general flow.

Experiment  $f_2$  includes latent-heat flux from the sea, but not orography. The spatial distribution of precipitation obtained for the 12-hour forecast (not shown) is very similar to that obtained from experiment  $f_0$  (Fig. 13(a)). In the  $f_2 - f_0$  precipitation field (not shown), only small differences appear to the east of the Balearic Islands and close to the Catalan coast. Both areas correspond to the limit of zones where evaporation and moisture advection are strong. We conclude that evaporation may be an important factor in such events, but not for periods as short as this simulation. Similarly, the effect of evaporation on the wind field is considered to be negligible.

The effect of the interaction between orography and evaporation from the sea on the precipitation field (not shown) is also weak. The largest positive effects in precipitation appear over the Catalan coast. They reveal some spatial redistribution, but they are not very significant. The effect on the wind field is also very weak, except over the sea close to the Catalan coast. This effect seems to act in the opposite sense to the orographic effect, and the major outcome is a small cyclonic circulation that appears on the western side of the Gulf of Lyons.

## 6. CONCLUSIONS

The results obtained from these experiments show that mesoscale models, with appropriate parametrizations for convection, can be used to study convective events involving heavy rain. The model that we were using gave results that approximated very well to the observed spatial distribution of precipitation over land. (It was not possible to verify the precipitation forecast over sea because there was no radar operating at that time in Catalonia and the Balearic Islands). However, the forecast of amount of precipitation was not so good because the model underestimated the rainfall. A qualitative comparison between the model results and the wind observations showed good correlation. The simulation also displayed some of the observed mesoscale features, such as, in particular, the Algerian low in the lee of the Atlas mountains, which help to deflect the flow at low levels towards Catalonia and so localize convection over that area.

The study of the effects of orography and evaporation from the sea showed that the effect of the former appears to be decisive in the spatial structure of precipitation over land, the orography being responsible for localizing the precipitation within the coastal zone. The effect of the orography on the wind field at low levels is also significant. The formation of a shallow cyclonic circulation over the sea, close to the Algerian coast, and the strong modification of the wind field close to Catalonia are due to the orography. Both these zones are connected by a convergence line which also is associated with the orography. The effect of evaporation from the sea on both precipitation and wind fields seems to be very weak. Perhaps with a longer simulation the effect of the evaporation might be more important. The combined effect of orography and evaporation on both fields is also weak. The effect on the wind field becomes important only close to the Catalan coast, through the formation of a very small cyclonic circulation.

More experiments need to be carried out to confirm and identify the effects of all these factors. Examples are available of heavy rain events lasting several days, which could help in assessing the effect of evaporation from the sea. The application of the numerical simulation technique to other events occurring in the Valencia or Murcia region could be of help in providing a discriminatory means of knowing where convection is likely to be located.

#### ACKNOWLEDGEMENTS

The authors gratefully acknowledge the assistance of the Meteorological Centre of Palma de Mallorca of the INM of Spain for providing the observational data and satellite images used in this work. The authors also thank Dr Kerry A. Emanuel (MIT) for his help in the inclusion of his convection scheme in the model, and Dr Charles A. Doswell III, who is visiting the UIB under grant SAB95-0136, for his review of the manuscript and critical comments. This work has been supported partially by grants EU EV5V-CT94-0442, CICYT AMB95-1136-CE and DGICYT PB94-1169C02-02.

#### REFERENCES

- Arakawa, A. and Schubert, W. H. 1974 Interaction of a cumulus cloud ensemble with the large-scale environment. Part I. *J. Atmos. Sci.*, **31**, 674–701
- Alpert, P., Tsidulko, M. and Stein, U. 1995 Can sensitivity studies yield absolute comparisons for the effects of several processes? *J. Atmos. Sci.*, **52**, 597–601
- Barnes, S. L. 1985 Omega diagnosis as a supplement to LFM/MOS guidance in weakly forced convective situations. *Mon. Weather Rev.*, **113**, 2122–2141
- Barnes, S. L. and Newton, C. W. 1986 Thunderstorm, morphology and dynamics. Pp. 75–112 in *Thunderstorms in the synoptic setting*, 2nd edition. Ed. E. Kessler, Univ. Oklahoma Press
- Benjamin, S. G. and Carlson, T. N. 1985 Some effects of surface heating and topography on the regional severe storm environment. Part I: Three-dimensional simulations. *Mon. Weather Rev.*, **114**, 307–329
- Bessemoulin, P., Bougeault, P., Genovés, A., Jansá A. and Puech, D. 1993 Mountain pressure drag during PYREX. *Beitr. Phys. Atmos.*, **66**, 305–325
- Bhumralkar, C. M. 1975 Numerical experiments on the computation of ground surface temperature in an atmospheric general circulation model. *J. Appl. Meteorol.*, **14**, 1246–1258
- Blackadar, A. K. 1976 Modelling the nocturnal boundary layer. Pp. 46–49 in *Proc. Third Symp. Atmospheric Turbulence, Diffusion and Air Quality*. American Meteorological Society
- Bougeault, P. and Lacarrère, P. 1989 Parameterization of orographic induced turbulence in a mesobeta scale model. *Mon. Weather Rev.*, **117**, 1872–1890
- Davies, H. C. 1976 A lateral boundary formulation for multilevel prediction models. *Q. J. R. Meteorol. Soc.*, **102**, 405–418
- Emanuel, K. A. 1991 A scheme for representing cumulus convection in large-scale models. *J. Atmos. Sci.*, **48**, 2313–2335
- Fernández, C., Gaertner, M. A., Gallardo, C. and Castro, M. 1995 Simulation of a long-lived meso- $\beta$  scale convective system over the Mediterranean coast of Spain. Part I: Numerical predictability. *Meteorol. Atmos. Phys.*, **56**, 157–179
- Font, I. 1983 *Climatología de España y Portugal*. Instituto Nacional de Meteorología, Madrid
- Fritsch, J. M. and Chappell, C. F. 1980 Numerical prediction of convectively driven mesoscale pressure systems. Part I: Convective parameterization. *J. Atmos. Sci.*, **37**, 1722–1733
- García-Dana, F., Font, R. and Rivera, A. 1982 'Meteorological situation during the heavy rain event in the eastern zone of Spain during October-82.' Instituto Nacional de Meteorología, Madrid
- Jansá, A., Ramis, C. and Alonso, S. 1986 The Mediterranean thunderstorm on 15 November 1985: triggering mechanism. (In Spanish). *Rev. Meteorol.*, **8**, 7–19.

- Louis, J. F. 1979 A parametric model of vertical eddy fluxes in the atmosphere. *Boundary-Layer Meteorol.*, **17**, 187–202
- Mahfouf, J. F., Richard, E. and Mascart, P. 1987a The influence of soil and vegetation on the development of mesoscale circulations. *J. Clim. Appl. Meteorol.*, **26**, 1483–1495
- Mahfouf, J. F., Richard, E., Mascart, P., Nickerson, E. C. and Rosset, R. 1987b A comparative study of various parameterizations of the planetary boundary layer in a numerical mesoscale model. *J. Clim. Appl. Meteorol.*, **26**, 1671–1695
- Mahrer, Y. and Pielke, R. A. 1977 The effects of topography on the sea and land breezes in a two-dimensional numerical model. *Mon. Weather Rev.*, **105**, 1151–1162
- Miró-Granada, J. 1974 Les crues catastrophiques sur la Méditerranée occidentale. *AMS-AISH Public.*, **12**, 119–132
- Nickerson, E. C., Richard, E., Rosset, R. and Smith, D. R. 1986 The numerical simulation of clouds, rain and airflow over the Vosges and Black Forest mountains: a meso- $\beta$  model with parameterized microphysics. *Mon. Weather Rev.*, **114**, 398–414
- Paccanella, T., Tibaldi, S., Buizza, R. and Scocciati, S. 1992 High-resolution numerical modelling of convective precipitation over northern Italy. *Meteorol. Atmos. Phys.*, **50**, 143–163.
- Pedder, M. A. 1989 Limited area kinematic analysis by a multivariate statistical interpolation method. *Mon. Weather Rev.*, **117**, 1695–1708
- 1993 Interpolation and filtering of spatial observations using successive corrections and Gaussian filters. *Mon. Weather Rev.*, **121**, 2889–2902
- Pinty, J. P. 1984 'Une méthode variationnelle d'ajustement des champs de masse et de vent.' Note 72 de l'I.O.P.G., Université de Clermont II
- Pinty, J. P., Mascart, P., Richard, E. and Rosset, R. 1989 An investigation of mesoscale flows induced by vegetation inhomogeneities using an evapotranspiration model calibrated against HAPEX-MOBILHY data. *J. Appl. Meteorol.*, **28**, 976–992
- Raymond, D. J. and Blyth, A. M. 1986 A stochastic model for nonprecipitating cumulus clouds. *J. Atmos. Sci.*, **43**, 2708–2718
- Ramis, C. and Romero, R. 1995 A first numerical simulation of the development and structure of the sea breeze in the island of Mallorca. *Ann. Geophys.*, **13**, 981–994
- Ramis, C., Jansá, A., Alonso, S. and Heredia, M. A. 1986 Convección sobre el Mediterráneo occidental: estudio sinóptico y observación remota. *Rev. Meteorol.*, **7**, 59–82
- Ramis, C., Llasat, M. C., Genovés, A. and Jansá, A. 1994 The October–1987 floods in Catalonia: Synoptic and mesoscale mechanisms. *Meteorol. Appl.*, **1**, 337–350
- Ramis, C., Alonso, S. and Llasat, M. C. 1995 A comparative study of two cases of heavy rain in Catalonia. *Surv. Geophys.*, **16**, 141–161
- Reiter, E. R. 1975 'Handbook for forecasters in the Mediterranean.' Naval Postgraduate School, Monterey, California
- Richard, E., Mascart, P. and Nickerson, E. C. 1989 The role of surface friction in downslope windstorms. *J. Appl. Meteorol.*, **28**, 241–251
- Romero, R., Alonso, S., Nickerson, E. C. and Ramis, C. 1995 Influence of vegetation on the development and structure of mountain waves. *J. Appl. Meteorol.*, **34**, 2230–2242
- Scofield, R. A. and Purdom, J. F. W. 1986 The use of satellite data for mesoscale analyses and forecasting applications. Pp. 118–150 in *Mesoscale Meteorology and Forecasting*. Ed. P. S. Ray. American Meteorological Society, Boston
- Shapiro, R. 1970 Smoothing, filtering and boundary effects. *Rev. Geophys. Space Phys.*, **8**, 359–387
- Stein, U. and Alpert, P. 1993 Factor separation in numerical simulations. *J. Atmos. Sci.*, **50**, 2107–2115
- Therry, G. and Lacarrère, P. 1983 Improving the eddy-kinetic energy model for planetary boundary-layer description. *Boundary-Layer Meteorol.*, **25**, 63–88
- Vergeiner, I., Steinacker, R. and Dreiseitl, E. 1982 The south foehn case 4/5 May 1982. Pp. 143–154 in *Alpex preliminary scientific results*. Ed. J. P. Kuettner, GARP-ALPEX, n 7, WMO
- Warner, T. T., Anthes, R. A. and McNab, A. L. 1978 Numerical simulations with a three-dimensional mesoscale model. *Mon. Weather Rev.*, **106**, 1079–1099